

# The bite angle makes the difference: a practical ligand parameter for diphosphine ligands

Peter Dierkes\* and Piet W. N. M. van Leeuwen

*Institute for Molecular Chemistry, Nieuwe Achtergracht 166, NL-1018 WV Amsterdam, The Netherlands*

*Received 7th October 1998, Accepted 5th February 1999*

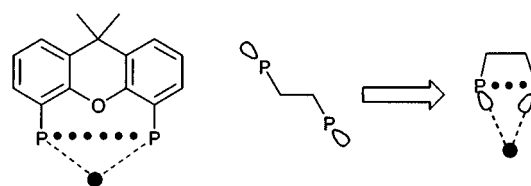
Over the past twenty years, a correlation between the P–M–P bite angle in diphosphine complexes and selectivity has been observed in various catalytic reactions such as hydroformylation, hydrocyanation and cross coupling. The large number of examples indicates that this correlation is not fortuitous. In order better to understand the underlying principles of the bite angle effect, we have first analysed crystal structures available in the Cambridge Crystallographic Database. Systematic searches indicate that for many bidentate diphosphine ligands the P–M–P angles concentrate in surprisingly small ranges, even if complexes of different metals in various oxidation states are considered. Several examples in the literature show that continuous electronic changes associated with changing bite angles cannot only be verified by different spectroscopic techniques, but also explained on a theoretical level (Walsh diagrams). The ligand bite angle is a useful parameter for the explanation of observed rates and selectivities and likewise for the design of ligands for new catalytic reactions.

## 1 Introduction

Homogeneous catalysis has reached a state of maturity that allows its application in organic synthesis and industry. The optimisation of known procedures and the efficient development of new catalytic systems call for a more systematic approach to ligand design. Several empirical ligand parameters have been suggested to predict catalyst performance. Many of them can help to understand qualitatively why a ligand leads to the observed rate and/or selectivity. A ligand parameter that can easily be evaluated from low-level computer modelling and/or systematic crystal structure analyses could be a valuable tool to determine which ligand to use for a reaction or how to

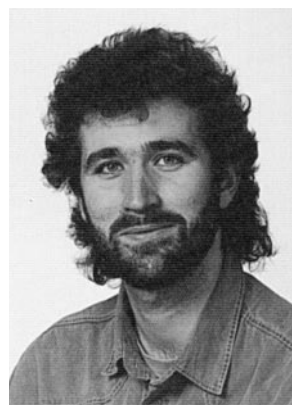
modify a given ligand to gain more control over a catalytic reaction. More than 1000 citations have been made in the last ten years to Tolman's review article<sup>1,2</sup> introducing the cone angle concept for phosphine ligands. A large number of studies have been reported since on more advanced parameters for (mono)phosphine ligands. Models using two or three parameters can be used to predict properties ranging from  $pK_a$  values to various spectroscopic properties of phosphines/phosphites and the corresponding metal complexes.<sup>3–5</sup>

While Tolman's cone angle concept is widely accepted for monodentate ligands, the extension to bidentate ligands appears to be less straightforward. Diphosphine ligands, however, offer more control over regio- and stereo-selectivity in many catalytic reactions. The major difference between mono- and bi-dentate ligands is the ligand backbone, a scaffolding which keeps two phosphorus donor atoms at a specific distance (Scheme 1). The distance is ligand specific and, together with



**Scheme 1** The P...P distance is determined by backbone constraints. It can be measured most easily as a standardised ligand bite angle using a dummy atom to ensure the right orientation of the two donor atoms.

the flexibility of the backbone, an important characteristic of a ligand. A standardised bite angle, with defined M–P bond lengths and a “metal” atom that does not prefer any specific P–M–P angle would appear to be the most convenient way of comparing bidentate ligands systematically.



Peter Dierkes

*Peter Dierkes studied chemistry at Münster University and Imperial College in London. After taking a Ph.D. in Professor Dehnicke's group in Marburg, Germany, 1994, he spent two years as a postdoc in Professor Osborn's laboratories in Strasbourg, and is currently working at the University of Amsterdam towards his Habilitation. Research interests include organometallic chemistry, the preparation of chiral ligands, mechanistic studies of catalytic reactions and molecular modelling on different levels of theory.*



Piet W. N. M. van Leeuwen

*Piet W. N. M. van Leeuwen is professor of homogeneous catalysis at the University of Amsterdam. He did his Ph.D. in co-ordination chemistry at the University of Leyden. He spent much of his career at Shell Research in Amsterdam. His research aims at the development of novel transition-metal homogeneous catalysts, using the full range of available tools and techniques.*

Of the large number of conformations “free” ligands can adopt, few contain the phosphorus atoms with the correct orientation to allow bidentate co-ordination to a single metal centre. The lone pairs of electrons have to point in the direction of the metal centre. The easiest way to find these conformations is the introduction of a dummy metal atom. If the same dummy–phosphorus bond length is used for all ligands, the calculated bite angles are a function of the non-bonded P···P distance. We will describe the “bite angles” obtained in this way as ligand bite angle, as opposed to P–M–P “bite” angles measured in crystal structures.

The evaluation of parameters affecting catalyst efficiencies is not always straightforward. Catalytic reactions are sequences of elementary reactions. Variation of a single parameter may promote one step but slow down another. Equilibria involving catalytically active species can be shifted by small changes in reaction conditions.<sup>6,7</sup> The overall effect may not be very characteristic.<sup>8</sup> The potential formation of different catalytic species has to be taken into account when a series of similar ligands are compared. With increasing ligand bite angles, the formation of *trans* complexes or dimeric species becomes more likely.<sup>9</sup> Increasing flexibility of a ligand backbone raises the chance of an arm-off  $\eta^1$  co-ordination. The latter may explain the sometimes drastically different efficiency of  $\text{Ph}_2\text{P}(\text{CH}_2)_4\text{PPh}_2$ , dppb, compared to  $\text{Ph}_2\text{P}(\text{CH}_2)_3\text{PPh}_2$ , dppp, observed in various reactions.

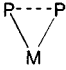
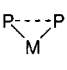
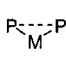
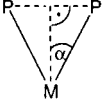
Despite these limitations, many examples show that the ligand bite angle is related to catalytic efficiency in a number of reactions. Early examples are the platinum–diphosphine–tin catalysed hydroformylation<sup>10,11</sup> or palladium catalysed cross coupling reactions of Grignard reagents with organic halides.<sup>12,13</sup> In recent years, a correlation between ligand bite angles and catalyst selectivities has been observed in rhodium catalysed hydroformylation,<sup>14–16</sup> nickel catalysed hydrocyanation<sup>17,18</sup> and even Diels–Alder reactions.<sup>19</sup> Some catalytic reactions, for example nickel–diphosphine catalysed hydrocyanation, only work if ligands with very large bite angles ( $>100^\circ$ ) are employed. In other reactions, high enantioselectivities with specific substrates require ligands with large bite angles.<sup>20–22</sup>

The P–M–P angle found in transition metal complexes is a compromise between the ligand’s preferred bite angle and the one preferred by the metal centre. The former is mainly determined by constraints imposed by the ligand backbone and by steric repulsion between substituents on the phosphorus atoms and/or the backbone. Electronic effects seem to have a more indirect influence by changing the preferred metal–phosphorus bond length. The metal preferred bite angle, on the other hand, is mainly determined by electronic requirements, *i.e.* the nature and number of d orbitals involved in forming the molecular orbitals. Other ligands attached to the metal centre can influence the bite angle if they are very bulky or if they have a strong influence on the metal orbitals ( $\pi$ -bonding ligands for example).

Ligands enforcing unusually small or large bite angles have long been employed to synthesize transition metal complexes that are not stable when ligands with classic ligand bite angles are used.  $\pi$  Complexes with dioxygen are an early example,<sup>23</sup> and Hofmann *et al.*<sup>24</sup> synthesized  $[\text{Ni}\{\eta^2\text{-(C,O)-Ph}_2\text{C=C=O}\}(\text{P-P})]$  (P–P = bidentate diphosphine) complexes after correctly predicting an increasing stability of  $\eta^2\text{-(C,O)}$  compared to  $\eta^2\text{-(C,C)}$  co-ordination with decreasing bite angles.

For the calculation of ligand bite angles, either molecular modelling or P···P distances determined from crystal structures can be used. Molecular modelling has been used to calculate “natural” bite angles, ligand bite angles calculated using a “rhodium” dummy atom and fixed Rh–P distances of 2.315 Å.<sup>25</sup> Crystallographic data can be retrieved from the Cambridge Crystallographic Database. With the large number of crystal structures available, average values can be calculated for many ligands. This decreases errors due to packing effects or other

**Table 1** The bite angle of a ligand with a given P···P distance strongly depends on the M–P bond length: the bite angle for a defined bond length can be calculated from the P···P distance [ $\text{P–M–P} = 2\arcsin(r_{\text{P}\cdots\text{P}}/2r_{\text{M–Pnew}})$ ] or a measured bite angle and the M–P-distances  $r_{\text{P}\cdots\text{P}}$  is the P···P distance and  $\text{M–P}_{\text{new}}$  the new bond length]

			
$r_{\text{P}\cdots\text{P}} = 3.0 \text{ \AA}$ M–P = 2.4 Å P–M–P = 77.4°	$r_{\text{P}\cdots\text{P}} = 3.0 \text{ \AA}$ M–P = 2.3 Å P–M–P = 81.4°	$r_{\text{P}\cdots\text{P}} = 3.0 \text{ \AA}$ M–P = 2.2 Å P–M–P = 86.0°	$\alpha = \angle \text{P–M–P}/2$ $\sin \alpha = (1/2 r_{\text{P}\cdots\text{P}})/r_{\text{M–P}}$

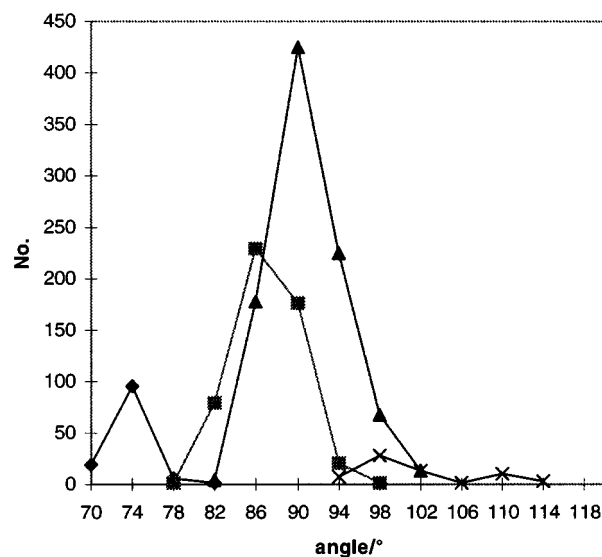


**Fig. 1** Number of (P–P)M fragments with P–P = dppm (◆), dppe (■), dppp (▲) and dppf (×) found in a CSD search. For details of structure searches see Table 2.

“errors” in the crystal structures. Bite angles are a function of the M–P bond length. In order to obtain a meaningful comparison between different ligands, the measured (or calculated) angles have to be standardised to one, defined M–P bond length. Standardised bite angles can be calculated from the P···P distance (Table 1).

In the following, a discussion of ligand and metal preferences for certain bite angles will be followed by examples illustrating the use of similar ligands with different bite angles in various catalytic reactions.

## 2 The ligand preferred bite angle

### Statistical analyses of crystal structures

The examination of crystal structures is a good starting point to gain more insight into ligand and metal preferences contributing to the actually measured bite angle. The P–M–P bite angles of transition metal complexes containing (P–P)M fragments documented in the Cambridge Crystallographic Database CSD have been examined for a series of bidentate diphosphine ligands P–P. No restrictions were imposed on the nature of the transition metal M, its oxidation state or other ligands co-ordinated to the same metal centre. The results are summarised in Table 2. Despite the rather crude filtering,<sup>26,27</sup> the angles concentrate in a narrow range for most ligands; the standard deviations, a measure for the broadness of a distribution around the mean value, lie between 1.5 and 3° (see Fig. 1). The standard deviations are similar to those Müller and Mingos<sup>28</sup> found for Tolman cone angles of monophosphine ligands. This is remarkable, as one would expect ligands with

**Table 2** Diphosphine ligand bite angles ( $^{\circ}$ ) calculated with force field methods compared to average P–M–P angles calculated from crystal structures retrieved from the CSD

Ligand	P–M–P <sub>2.315</sub> <sup>a</sup> / $^{\circ}$	X-ray, average value		Molecular modelling, $\beta_n$ / $^{\circ}$
		P–M–P/ $^{\circ}$	$r_{M-P,av}$ (CSD)/ $\text{\AA}$	
dppm	71.71 (1.60)	71.53 (2.44)	2.32 (0.09)	
dpp-benzene	83.04 (2.73)	81.95 (3.25)	2.34 (0.12)	
dppe	85.03 (3.11)	82.55 (3.65)	2.38 (0.13)	78.1, <sup>b</sup> 84.4 (70–95) <sup>c</sup>
dppe-Bu <sup>d</sup>	87.23 (1.26)	89.74 (2.49)	2.27 (0.06)	
dppp	91.08 (4.00)	91.56 (3.70)	2.29 (0.09)	86.2 <sup>b</sup>
dppp-Me <sup>d</sup>	89.87 (3.86)	90.51 (2.27)	2.30 (0.06)	
dppp-Bu <sup>d</sup>	99.33 (0.74)	100.35 (1.53)	2.30 (0.02)	
dppb	97.70 (5.15)	97.07 (2.84)	2.38 (0.11)	98.6 <sup>b</sup>
dppf	95.60 (4.34)	98.74 (3.42)	2.26 (0.07)	
BINAP	92.43 (2.6)	92.77 (1.95)	2.31 (0.04)	
DIOP	97.63 (4.72)	100.0 (4.3)	2.28 (0.02)	102.2 (90–120) <sup>f</sup>
DUPHOS-Me	82.61	84.7 <sup>68</sup>	2.27	
BISBI	122.18 (14.35)	119.64 (43.48)	2.34 (0.12)	122.6 (101–148) <sup>f</sup> 112.6 (92–155) <sup>c</sup> 123 (110–145) <sup>c</sup> 111.2 <sup>h</sup>
NORPHOS				107.6 (93–131) <sup>c</sup>
TRANSPHOS		104, 131.9, 175.7 <sup>g</sup>		102.2 (86–120) <sup>f</sup>
T-BDCP				111.7 (97–135) <sup>f</sup>
DPEphos	102.51	101.46 <sup>i</sup>	2.33 <sup>i</sup>	109.4 (94–130) <sup>f</sup>
Xantphos	107.12	104.64 <sup>i</sup>	2.36 <sup>i</sup>	108.7 (93–132) <sup>f</sup>
Thixantphos				131.1 (117–147) <sup>f</sup>
Sixantphos	105.36	104.28 <sup>i</sup>	2.34 <sup>i</sup>	
DBFphos				

The bite angles given are based on crystal structure data retrieved from the October 1997 version of the CSD. The data have been filtered: the structure contains a d- or f-block metal, “ $R \leq 10$ ”, the “error free” and the “no disorder” options were enabled, and the coordinates had to be available in the database. If a structure contained a complex with more than one diphosphine ligand bound to a metal centre, or if more than one molecule was present in an elementary cell, or if a structure was determined more than once, all entries were processed. Ligands carrying substituents other than H on the phenyl rings or the bridge and ligands with a mono- or tri-dentate co-ordination have not been used. The structures of the ligands are shown in Tables 3 and 4. For crystal structure data, the values given in parentheses are the standard deviations; for modelled bite angles they indicate the range of bite angles a ligand can accommodate with no more than 3 kcal mol<sup>-1</sup> strain energy (flexibility range). <sup>a</sup> Standardised ligand bite angle with M–P distances of 2.315 Å calculated from the P···P distance as found in the CSD  $\{=2\arcsin^2(r_{P\dots P}/2.315)\}$ . <sup>b</sup> Ref. 63. <sup>c</sup> Ref. 14. <sup>d</sup> dppe-Bu = <sup>t</sup>Bu<sub>2</sub>P(CH<sub>2</sub>)<sub>2</sub>P<sup>t</sup>Bu<sub>2</sub>, dppp-Me = Me<sub>2</sub>P(CH<sub>2</sub>)<sub>3</sub>PMe<sub>2</sub>, and dppp-Bu = <sup>t</sup>Bu<sub>2</sub>P(CH<sub>2</sub>)<sub>3</sub>P<sup>t</sup>Bu<sub>2</sub>. <sup>e</sup> Averages calculated excluding structures of tetrahedral nickel(II) complexes [*ca.* 104°,  $r_{M-P} \approx 2.30$  Å] and complexes of Cu<sup>I</sup>, Ag<sup>I</sup> and Au<sup>I</sup> with d<sup>10</sup> metal centres 111.42° (2.47) ( $r_{M-P}$  2.32 Å), see Fig. 2]. <sup>f</sup> Ref. 15. <sup>g</sup> Cited in ref. 25. <sup>h</sup> Calculated from 112.3°<sup>25</sup> with a Rh–P distance of 2.30 Å. <sup>i</sup> Bidentate co-ordination with no M–O interaction.<sup>32</sup>

flexible backbones, such as dppb, to adopt large ranges of bite angles.

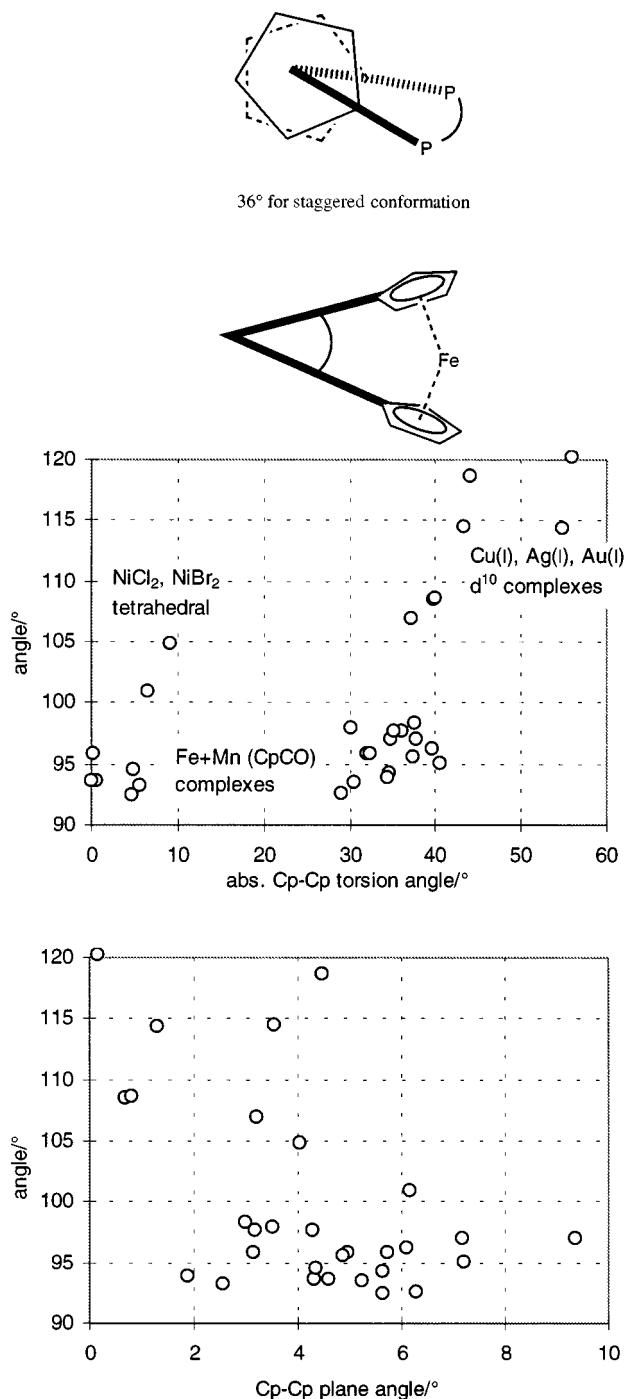
The narrow distribution of bite angles observed in mono-nuclear complexes are an indication that the P–M–P angle in monomeric complexes containing (P–P)M fragments with small P–M–P angles is predominantly determined by the P···P distance defined by the ligand backbone. If a (P–P)M complex is formed the measured bite angle reflects the ligand preferences rather than the metal requirements. If metal and ligand requirements do not match di- or poly-nuclear complexes are formed preferentially. Ligands with bite angles above 100° appear to be more flexible. Unfortunately, the number of crystal structures with these ligands is too small to allow a meaningful statistical treatment. The good agreement, however, between the ligand bite angles obtained from molecular modelling and the normalised P–M–P angles found in crystal structures is encouraging. Caution should be applied when ligands with potential donor atoms in the backbone are analysed. Weak interactions between a third ligand atom and the metal centre with M–X distances around 3 Å can lead to considerably larger P–M–P angles in crystal structures (even above 150°) of dppe<sup>29</sup> or Xantphos-type<sup>30</sup> ligands.

An example may help to illustrate the contributions of the metal and the ligand preferences to the observed bite angle. A more detailed analysis of the angles found for 1,1'-bis(diphenylphosphino)ferrocene (dppf) ligands yielded interesting results. The ferrocene backbone is generally assumed to be very flexible: the bite angle can be increased by either opening the angle between the two Cp planes or by increasing the torsion angle along the axis described by the two centroids of the Cp rings.<sup>31</sup> Fig. 2 illustrates that, in most complexes, the bite angle is determined by the ligand preference, roughly 96°. This corresponds to a nearly coplanar orientation of the cyclopentadienyl

rings with a staggered conformation (“ideal” staggered torsion angle 36°). If, however, the metal has a strong preference to form other angles the ligand will adapt to them. The angles of 102 and 105° found for tetrahedral nickel complexes are roughly the average values between ligand (96°) and metal (tetrahedral angle 109°) preferences. Complexes of Cu<sup>I</sup>, Ag<sup>I</sup> and Au<sup>I</sup> and other d<sup>10</sup> metal ions have a strong tendency to form linear (L–M–L 180°) or trigonal planar (L–M–L 120°) geometries. The Walsh diagram (see below) indicates a sharp increase of energy with decreasing bite angles. Consequently, the bite angles are larger. Interestingly, the average M–P distance (2.34 Å,  $\beta_{2.315} = 111.65^{\circ}$ ) is not significantly different to that in other dppf complexes (2.32 Å,  $\beta_{2.315} = 99.33^{\circ}$ ). This can be interpreted in terms of flexibility of the ferrocene backbone. A study of palladium–TCNE complexes with different ligands based on the more rigid xanthene based backbone shows that elongation of the Pd–P bond is another way of compromising between the ligand and the metal preferred bite angle.<sup>32</sup>

### Bite angles from computer modelling

Computer modelled geometries can be used to estimate ligand bite angles. The obvious advantage is that no crystal structure is required. The calculations can even be performed before ligands are synthesized. If computer modelling is employed to design new ligands it is more important to calculate a correct trend rather than perfect geometries. Bite angles of all ligands in a series should thus be modelled with the same program and the same parameter set. Various molecular modelling packages using different force fields and force field parameters have been used to calculate ligand bite angles. For the Xantphos ligand (Table 3), the structure calculated with force field methods was found to be closer to the crystal structure than that obtained

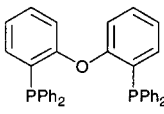
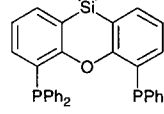
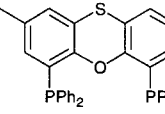
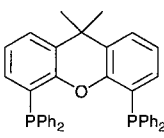
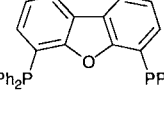
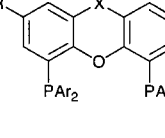
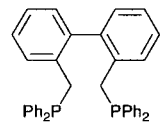
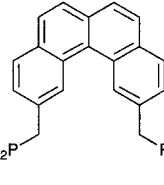
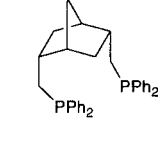
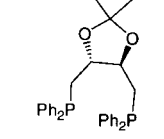
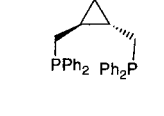
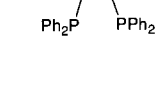


**Fig. 2** Distribution of ligand bite angles vs.  $C_{ipso}$ -centroid-centroid- $C_{ipso}'$  torsion for transition metal-1,1'-bis(diphenylphosphino)ferrocene complexes found in the CSD. The torsion angles indicated are absolute values retrieved from the CSD. The distance between the centroids of the two cyclopentadienyl rings has been constrained to  $3 < r < 3.5$  Å to exclude values for  $\eta^1$ -bound dppf ligands (average value in  $\eta^2$ -bound dppf ligands 3.287, minimum 3.206, maximum 3.327, standard deviation 0.02 Å). In most complexes the dppf ligand assumes a staggered conformation with a bite angle around  $96^\circ$  and a torsion angle between 30 and  $40^\circ$ ; the torsion angle for the staggered conformation of ferrocene is  $36^\circ$ . Interestingly, the angle between the two Cp rings decreases with increasing bite angle.

with AM1 or PM3 semiempirical calculations.<sup>32</sup> The force field parameters available for the ligand part of transition metal diphosphine complexes are sufficiently good for our purposes.

The parameterisation of a metal atom in a transition metal complex with several different ligands bound to the central core is more difficult. A closer examination of the force field parameters that have been used to calculate bite angles of diphosphine

**Table 3** Ligand bite angles calculated by molecular modelling, within parentheses the range accessible with  $\Delta E$  calculated to be  $\leq 3$  kcal mol<sup>-1</sup> (flexibility range)

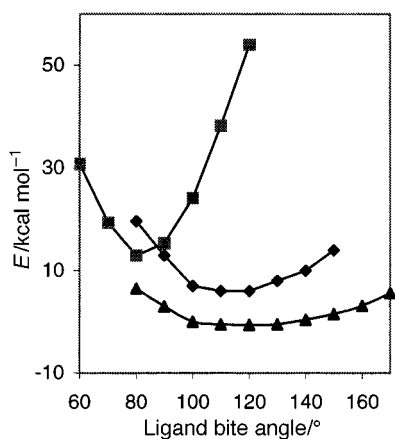
 DPEphos 102.2° (86-120°) <sup>a</sup>	 Sixantphos 108.7° (93-132°) <sup>a</sup>	 Thixantphos 109.4° (94-130°) <sup>a</sup>
 Xantphos 111.7° (97-135°) <sup>a</sup>	 DBFphos 131.1° (117-147°) <sup>a</sup>	 generic structure
 BISBI 112.6° (92-155°) <sup>b</sup>	 TRANSPHOS 111.2° <sup>c</sup>	 NORPHOS 123° (110-145°) <sup>b</sup>
 DIOP 102° (90-120°) <sup>b</sup>	 T-BDCP 107.6° (93-131°) <sup>b</sup>	 dppe 84.4° (70-95°) <sup>b</sup>

Values calculated or cited in: <sup>a</sup> ref. 15; <sup>b</sup> ref. 14; <sup>c</sup> see Table 2. The original authors have used rhodium as a “dummy metal atom” ( $r_{Rh-P} = 2.315$  Å) and the Sybyl (Tripos force field)<sup>a</sup> or MacroModel (Amber force field)<sup>b,c</sup> program packages to calculate the angles.

ligands in rhodium complexes<sup>15,25</sup> shows that the rhodium atom is effectively reduced to a “dummy metal atom”. The force constant for the P–M–P bond angle is reduced to 0, and a high energy constraint fixes the “Rh”–P bond length to 2.315 Å, a typical distance found in crystal structures. Despite the strongly simplified parameters, the agreement of the calculated ligand bite angles with average values from crystal structures is very good (Table 2). The metal atom cannot be eliminated completely. A “dummy metal atom” is necessary to pull the lone pairs of electrons and the substituents on the phosphorus atoms in the right direction and to simulate the constraints imposed on the ligand backbone by the metal atom in a complex, more precisely the effect of two M–P bonds with a given length and orientation (Scheme 1).

It may be useful to keep some points in mind when estimating ligand geometries using force field methods: many programs tend to overestimate attractive coplanar  $\pi$ -stacking interactions of aromatic groups and repulsive interactions of alkyl groups on the ligand. Ligand bite angles may thus be calculated as being too small in structures with coplanar phenyl groups on the two phosphorus atoms (e.g. dppe) and too large for ligands carrying bulky alkyl substituents. Owing to leverage effects, small errors in the backbone geometry can lead to larger errors in the calculated ligand bite angle.

A second parameter can be used to describe the rigidity of the ligand backbone: Casey defined a “flexibility range”,<sup>25</sup> the range of bite angles a ligand can adopt if conformations with energies slightly above that of the minimised structure are considered. It can be estimated from a computed potential energy



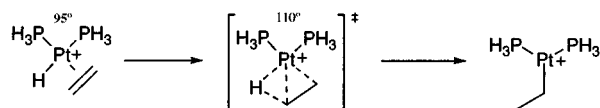
**Fig. 3** Calculated (Sybyl 6.4) flexibility of the DUPHOS (■), Xantphos (◆) and BISBI (▲) ligands. The flexibility range is determined by calculating the energy of structures minimised with constrained P–M–P angles.

diagram. The flexibility range has been defined as the range of bite angles accessible within 3 kcal mol<sup>-1</sup> of the minimum energy. Fig. 3 shows the energies of three ligands as a function of the bite angle. The values are calculated by minimising the energies of a series of structures with the P–M–P angle constrained to different values. A steeper curve indicates a less flexible ligand. Interestingly, the distribution of bite angles in crystal structures is indeed broader for ligands with a larger calculated flexibility range (Table 1).

### 3 The metal preferred bite angle

It is important to know the “preferred” bite angles of crucial intermediates in the catalytic cycle to decide which ligands to use for a catalytic reaction. A first approach can be based on complex geometries. In a rough approximation, the metal preferred bite angle for *cis*-co-ordinated bidentate ligands is 90° in a square planar or octahedral complex, 109° in a tetrahedral complex and 120° for the bis-equatorial co-ordination in a trigonal-bipyramidal complex. These geometries are frequently found for intermediates in reactions catalysed by diphosphine-transition metal complexes. The metal preferred bite angle changes during a catalytic reaction. For a more accurate indication of metal preferred bite angles, structures calculated by high-level computer modelling are useful. Most complexes modelled by *ab initio* or density functional methods have been extremely simplified in order to reduce the computation time necessary to optimise the structures. This is an advantage for this discussion. In “real” complexes the ligand positions are determined by a mixture of metal orbital requirements and inter-/intra-ligand steric interactions. Bulky ligands require space. In modelled structures, with protons representing the bulky groups, steric interactions are limited. The position of the PH<sub>3</sub> ligands is consequently a very good indication of metal orbital preferences.

An early (1978) and very good example to illustrate the value of computer modelled structures is the calculation of energies for Pt-group metal–diphosphine complexes as a function of the P–M–P angle. Thorn and Hoffmann<sup>33</sup> analysed the addition of hydrogen to ethylene catalysed by platinum diphosphine complexes (Scheme 2). Extended Hückel calculations showed a bite angle increasing from 95° in the olefin–hydride complex to 110°



**Scheme 2** The platinum-catalysed hydrogenation of ethylene calculated by Thorn and Hoffmann.<sup>33</sup>

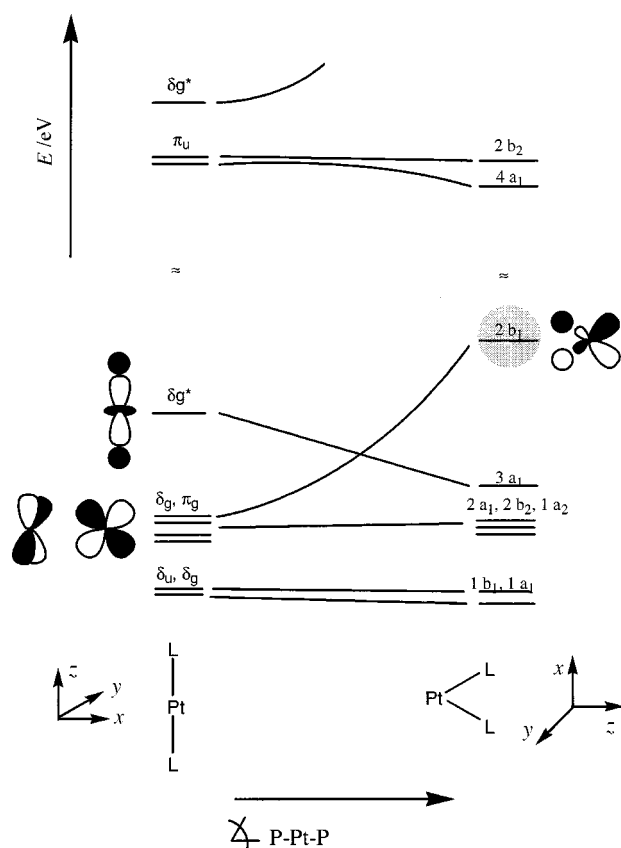
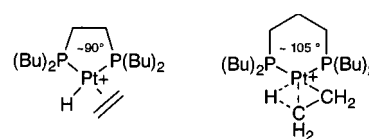


**Fig. 4** Walsh diagram for PtL<sub>2</sub> complexes with predominantly σ-bond ligands L. Reprinted from ref. 36 with permission from Elsevier Science.

in the transition state during the insertion of the hydride ligand into the Pt–C bond. The implied conclusion is that ligands with bite angles around 110° should stabilise intermediates between the η<sup>2</sup>-olefin complex and the η<sup>1</sup>-ethyl complex. Recent calculations on *ab initio*/density function levels indicate a bite angle around 101° in the transition structure.<sup>34</sup>

Thirteen years after Hoffmann’s original publication ethene–hydride and agostic ethyl complexes were indeed isolated: “The size of the chelating diphosphine ligand is shown to control the extent of transfer of a hydrogen atom from the β-carbon of the coordinated ethyl group to platinum with the smaller diphosphines favouring transfer to the metal.” A P–Pt–P angle of 104.8° was determined in the crystal structure of [Pt(η<sup>3</sup>-H-ethylene)(dppp-Bu)]<sup>+</sup> (Scheme 3). This complex is indeed an



**Scheme 3**

intermediate between an olefin–hydride complex and the alkyl complex, the product of a hydride insertion reaction.<sup>35</sup>

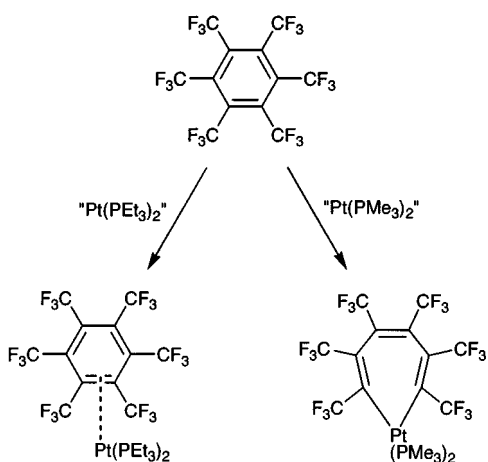
The relationship between the P–M–P bite angle and electronic properties of the metal centre has been investigated since by several authors. In transition metal complexes the symmetry of the molecular orbitals and the extent to which atomic orbitals contribute to them depends on the angle between the ligands. Walsh diagrams are a convenient way to visualise the energy of the molecular orbitals as a function of the P–M–P angle. A qualitative diagram calculated by Otsuka<sup>36</sup> (Fig. 4) for example helps to understand the preferred geometries in L–Pt<sup>0</sup>–L and L–Pt<sup>II</sup>–L complexes with predominantly σ-bonding ligands L. In d<sup>10</sup> complexes with monodentate ligands five MOs are occupied. The sum of their energies is lowest if the L–Pt–L

angle is close to 180°. If two electrons are removed, the  $\delta_g^*/2b_1$  orbital is empty. The  $d_8$  complexes thus prefer a geometry with  $3a_1$  being the HOMO.

If the L–Pt–L angle in a  $d^{10}$  complex is constrained to close to 90° the energy of the electrons in the non-bonding  $2b_1$  orbital is very high and the reduction potential of the complex is raised considerably.

The energy diagram explains why linear geometries are preferred by  $d^{10}$  and square-planar ones by  $d^8$  metal centres. The relation between the energy of the two electrons in the non-bonding orbital and the bite angle is nicely demonstrated when [PtCl<sub>2</sub>(P–P)] complexes are reduced with sodium amalgam in thf. If two (*t*-Bu)<sub>2</sub>P units linked by a (CH<sub>2</sub>)<sub>3</sub> chain (P–M–P<sub>2.315</sub> 99°) are employed a dimeric complex with a weak Pt–Pt bond is obtained. If the ligand bite angle is reduced by employing a (CH<sub>2</sub>)<sub>2</sub> spacer (P–M–P<sub>2.315</sub> 87°) “the enhanced reactivity of the [Pt(P–P)] species precludes formation of the dinuclear compound.” The dihydride complex isolated instead is probably the product of the reaction with thf.<sup>36</sup>

Peter Hofmann<sup>39</sup> has used Walsh diagrams to explain the different reactivity of platinum bis(phosphine) complexes {generated *in situ* from [Pt(PEt<sub>3</sub>)<sub>3</sub>] and [Pt(PMe<sub>3</sub>)<sub>2</sub>(PhCH=CHPh)], respectively} towards hexakis(trifluoromethyl)benzene. The unit [Pt(PEt<sub>3</sub>)<sub>2</sub>] forms an  $\eta^2$  adduct,<sup>37</sup> whereas [Pt(PMe<sub>3</sub>)<sub>2</sub>] inserts into the aromatic ring to form a seven-membered metallacyclic ring (Scheme 4).<sup>38</sup> Hofmann explains the different reac-



Scheme 4

tivities with a Walsh diagram very similar to the one shown in Fig. 4. The energy of the  $b_2$  orbital increases with decreasing P–M–P angle while that of the  $3a_1$  orbital decreases at the same time. The smaller cone angle of PMe<sub>3</sub> corresponds to a smaller P–Pt–P angle in the complex. According to Fig. 4, the energy of the  $\pi$ -symmetric  $b_2$  orbital should be higher, and the energy of the  $\sigma$ -symmetric  $3a_1$  orbital lower than for the PEt<sub>3</sub> complex. More electrons will consequently move from the ligand C–C  $\sigma$  bond to the empty  $4a_1$  orbital, and the 2 electrons occupying the  $2b_1$  orbital in the neutral platinum(0) complex move towards the ligand  $\pi^*$  orbitals when the complex is formed. The overall effect is a weaker ligand C=C bond due to electrons “moving” from the  $\sigma$  to the  $\pi^*$  orbital. In the PMe<sub>3</sub> complex this electron migration is strong enough to break the bond. The C<sub>6</sub>(CF<sub>3</sub>)<sub>6</sub> ring is opened to form the observed metallacycle.<sup>39</sup>

Even though tridentate ligands are used in the following example, the conclusions are very similar to those discussed for diphosphine complexes. Dubois and co-workers<sup>40</sup> examined the acidity of the hydride ligand and the catalyst activity in [Pd(H)(P–P–P)] complexes [P–P–P = Ph<sub>2</sub>P(CH<sub>2</sub>)<sub>n</sub>PPh(CH<sub>2</sub>)<sub>m</sub>–PPh<sub>2</sub>, *n, m* = 2 or 3]. Extended Hückel calculations indicate that, in diphosphine complexes with small ligand bite angles, electron density is shifted onto the hydride ligand. With increasing ligand bite angles the hydride ligand becomes more acidic. The

results can, qualitatively, be understood with the same Walsh diagram (Fig. 4).

Finally, the higher energy of the non-bonding electron pair in the resulting  $d^{10}$  complexes with smaller ligand bite angles explains the relationship between bite angles and the ease of oxidative addition<sup>41</sup> and reductive elimination<sup>42</sup> reactions of palladium diphosphine complexes (see below).

#### 4 Spectroscopic and electrochemical changes related to bite angles

The changes of energy levels associated with changes in ligand bite angles can also be measured directly. Changing energy levels should lead to changes in the spectroscopic properties of the metal complexes. Even though the qualitative discussion above does not allow quantitative predictions, consistent trends can be expected if a series of similar ligands is investigated. The absorption maxima in UV spectra of the  $\pi$ – $\pi^*$  transition of (dpmm, dppe, dppp) platinum 7,8-benzoquinoline complexes are blue-shifted with increasing ligand bite angles. The emission lifetime measured at 77 K increases in the same order.<sup>43</sup> In a study of nickel and palladium [M(P–P)<sub>2</sub>][BF<sub>4</sub>]<sub>2</sub> complexes the UV/vis absorption maximum  $\lambda_{\text{max}}$  and the half-wave potential  $E_1$  (Ni<sup>III</sup>, Pd<sup>II,0</sup>) were found to increase with the ligand bite angle.<sup>44</sup> These examples show that the effect of the ligand bite angle on a metal centre can indeed be measured directly by spectroscopy. The most impressive examples are recent correlations of transition metal NMR spectra with ligand bite or with Tolman angles. Metal NMR shifts can be a sensitive probe to electronic changes on a metal centre.<sup>45</sup> The <sup>103</sup>Rh NMR shift of a series of [Rh(hfacac)(P–P)] (hfacac = hexafluoroacetylacetonate) complexes is related to the P–Rh–P bite angles in a direct linear correlation.<sup>46</sup> The <sup>103</sup>Rh signal is shifted downfield with increasing ligand bite angle. This is a direct proof for the electronic effect of ligand bite angles. A correlation between metal NMR shifts and another ligand parameter has previously been observed for Tolman cone angles of mono-phosphine/-phosphite ligands and <sup>187</sup>Os/<sup>57</sup>Fe NMR shifts in  $\eta^6$ -arene-osmium or cyclopentadienyliron complexes respectively.<sup>47,48</sup>

#### 5 Ligand bite angles and reaction energy profiles

A ligand with a restrained ligand bite angle can be expected to change the energy profile of a reaction. During oxidative addition, insertion or reductive elimination reactions the coordination number of the metal centre and consequently the L–M–L angle changes. The angle of the transition state is likely between that of the reactant and that of the product complex. Enzymes often provide “pockets” which force the substrate into a transition state-like geometry. Even though most ligand backbones do not really change the substrate geometry considerably, they can force the catalyst into a transition state-like shape.

If a ligand bite angle is constrained to a value close to that expected for the transition state of a reaction the energy of the reactant complex is higher than that of an unrestrained complex. The energy of the transition state should be relatively unaffected and the activation energy for this step should be lower. The reaction step is accelerated and, if it is rate determining, the catalytic cycle runs more smoothly with a higher frequency. The reverse is true if the ligand bite angle is close to that of the reactant or product complex. The energy of the transition state will be higher, and the energy of the starting material is less affected. Owing to the increased activation energy<sup>49</sup> the reaction is slower (Fig. 5).

A good example is the nickel catalysed hydrocyanation of olefins (Scheme 5). With monophosphine ligands square-planar nickel dicyanides are formed (P–Ni–P *ca.* 90°) and the catalyst deactivates. If diphosphine ligands with large ligand bite angles are used the catalytic pathway is favoured.<sup>17,18</sup>

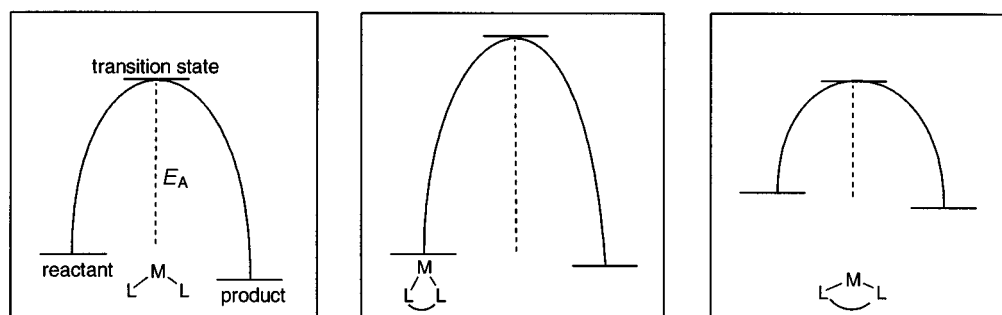
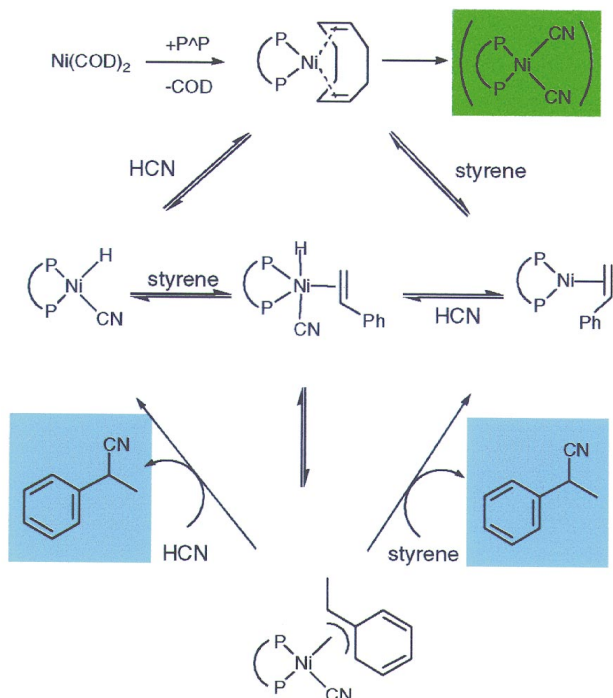


Fig. 5 The activation energy (dotted line) as a function of the L–M–L bite angle (qualitative picture).



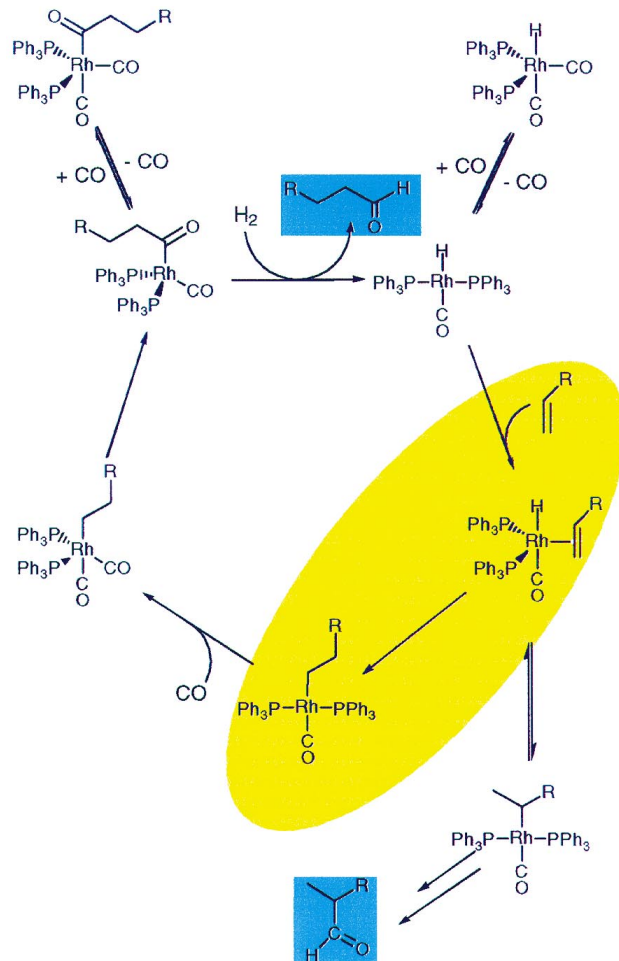
Scheme 5 Simplified catalytic cycle of the nickel catalysed hydrocyanation reaction.

## 6 Bite angle effects in catalysis

### Hydroformylation

The hydroformylation reaction is one of the most important applications of homogeneous catalysis in industry. From the first rhodium–phosphine catalysts found by Wilkinson and co-workers in the late sixties<sup>50,51</sup> it was only a short step to their application in industry (Scheme 6). Higher activities and selectivities obtained using rhodium catalysts compared to cobalt catalysts more than compensate the higher price of rhodium; cobalt catalysts are still widely used for the hydroformylation of  $> C_4$  olefins. The development of catalysts with even higher selectivities is one of the goals of current research in this area. While the thermodynamically favoured products are branched aldehydes, linear aldehydes are commercially more interesting.

In 1987 Kodak Eastman patented a BISBI-based rhodium catalyst with a high selectivity towards linear aldehydes.<sup>52</sup> To explain the selectivity, Casey and Whiteker<sup>25</sup> looked at bite angles of several ligands that form catalysts with a preference for linear aldehydes. They found a very good correlation between the ligand bite angle and the catalyst selectivity (Fig. 6).<sup>14</sup> Ligand (natural) bite angles were the basis of the first series of ligands developed by molecular modelling in our group. The members of the Xantphos family have a rigid backbone in common, which keeps the two phosphorus donor atoms at a distance of typically around 4 Å, corresponding to ligand bite angles between 100 and 130°. The ligands have very similar



Scheme 6 Simplified catalytic cycle of the rhodium catalysed hydroformylation reaction.

electronic properties. Table 4 summarises the results of hydroformylation reactions with 1-octene as a substrate. The correlation between the ligand bite angles and the selectivity is good. The selectivity towards the linear aldehyde is even higher than that of the system using BISBI.<sup>15</sup>

The reason for the correlation between the ligand bite angle and catalytic selectivity is the subject of an ongoing discussion. The first hypothesis was that a bis-equatorial co-ordination of the diphosphine ligand in a trigonal-bipyramidal intermediate increases the selectivity towards the linear product. The ideal angle for such a co-ordination is 120° (in a complex with the third ligand in the plane being similar to the other two).

Mechanistic studies have so far concentrated on the hydride insertion step (see Scheme 6). If a 1-alkyl intermediate is formed the linear aldehyde will result, whereas the 2-alkyl intermediate leads to the branched product (Fig. 7).

An explanation based purely on steric interactions was ruled



**Table 4** Hydroformylation of 1-octene at 40 °C:  $\beta_n$  is the calculated ligand bite angle (flexibility range in parentheses), t.o.f. the turnover frequency (mol alkene mol Rh<sup>-1</sup> h<sup>-1</sup>), hydrogenation products were not observed. Conditions: CO:H<sub>2</sub> = 1:1, substrate:Rh = 674:1, [Rh] = 1.78 mM. Data from ref. 15. The large bite angle of DBFphos probably prevents the formation of a monomeric (P-P)Rh complex

Ligand	$\beta_n^\circ$	Linear: branched	Product (%)		t.o.f.
			Linear	Isomerisation	
DPEphos	102.2 (86–120)	10.5:1	91.3	0	5
Sixantphos	108.7 (93–132)	35.0:1	96.3	<1	4.4
Thixantphos	109.4 (94–130)	47.6:1	97.0	1	13.2
Xantphos	111.7 (97–135)	57.1:1	98.3	0	10
DBFphos	131.1 (117–147)	3.4:1	76.1	1.6	1.9
BISBI	122.6 (101–148)	58.2:1	95.5	2.9	30

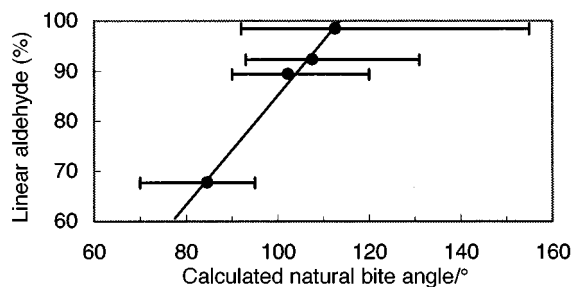


**Fig. 6** Hydroformylation of 1-hexene with rhodium–diphosphine complexes: plot of % *n*-aldehyde vs. calculated ligand bite angle of diphosphine (BISBI, T-BDCP, DIOP, dppe from top to bottom). Horizontal bars indicate the range of bite angles accessible with <3 kcal additional calculated strain energy. Reprinted with permission from ref. 14. Copyright 1992 American Chemical Society.

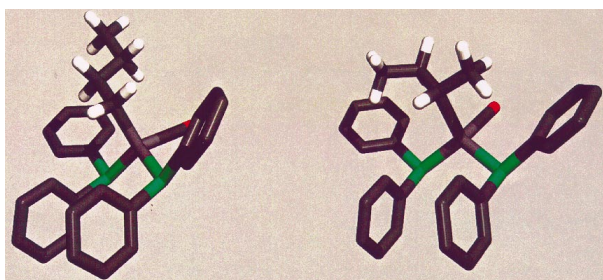


**Fig. 7** The current discussion on the selectivity determining step in hydroformylation reactions concentrates on the alkene addition step, the [Rh(CO)(alkyl)(P-P)] intermediate and the transition state of the hydride insertion reaction leading to its formation (P-P = Xantphos, backbone and hydrogen atoms omitted). The 1-alkyl chain (right) can avoid steric interactions more easily than the 2-alkyl group.

out because molecular mechanics energy calculations on “guessed” transition states for the hydride insertion step predict the wrong selectivities.<sup>53</sup> Similarly, a purely electronic explanation is unlikely. Hydroformylation experiments with electronically modified dppe, T-BDCP and BISBI ligands gave no conclusive picture.<sup>54</sup> Experiments with electronically modified Thixantphos ligands show that the ligand’s preference for a bis-equatorial co-ordination increases with decreasing phosphine basicity, while the regioselectivity is almost unaffected.<sup>56</sup>

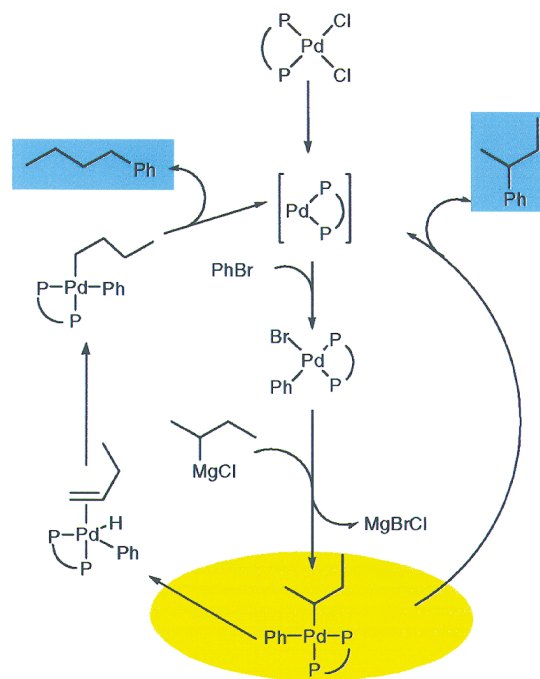
There are two preliminary conclusions. “The regioselectivity of hydroformylation is governed by a complex web of electronic and steric effects that have so far defied unraveling”,<sup>54</sup> and it may be possible that the regioselectivity is determined earlier in the cycle, namely the olefin addition to a four-co-ordinate [Rh(CO)H(P-P)] intermediate.<sup>55</sup>

### Palladium catalysed cross coupling reactions

Palladium catalysed cross coupling reactions are probably the most widespread examples for the application of homogeneous catalysis on a laboratory scale, and the industrial importance is growing rapidly. The broad range of coupling partners allows one to find conditions for almost any two reactants to be

coupled. While most reactions are performed with palladium complexes bearing monodentate phosphine ligands *e.g.* [Pd(PPh<sub>3</sub>)<sub>4</sub>], the use of bidentate ligands can enhance rate and/or selectivity.

As an example, the effect of diphosphine ligand bite angles (Table 5) on palladium catalysed cross coupling reaction of alkylmagnesium reagents with aryl halides has been studied by several authors. The reaction is assumed to begin with an oxidative addition of the aryl halide component to a zerovalent palladium–diphosphine species, followed by a transmetalation step that yields a [Pd(alkyl)(aryl)(P-P)] species. The cycle is closed by the reductive elimination of the alkylated aryl product (Scheme 7). Hayashi *et al.*<sup>12,13</sup> found an increased reaction



**Scheme 7** The catalytic cycle of a palladium catalysed Grignard cross coupling reaction.

rate with increasing ligand bite angles, dppe (P–M–P 85°) forming the slowest and least selective catalyst and dppf (P–M–P 96°) the best. The selectivity decreases again if ligands with bite angles above 102° are employed<sup>56</sup> (Table 6).

An aspect that has been neglected somewhat in the original papers is the strong dependence of the reaction rate on the ligand bite angle. In a first approach it is tempting to explain reaction rates with steric interactions between substrate and ligand. The larger the ligand bite angle the stronger is the substrate–ligand interaction (Scheme 8) and the slower the rate. However, the experiments show that the reverse is true. A closer examination of the reaction energy profile gives a likely explanation. Extended Hückel calculations<sup>49</sup> indicate a higher activation energy for the reductive elimination step if a diphosphine ligand bite angle is constrained to 90° compared to the



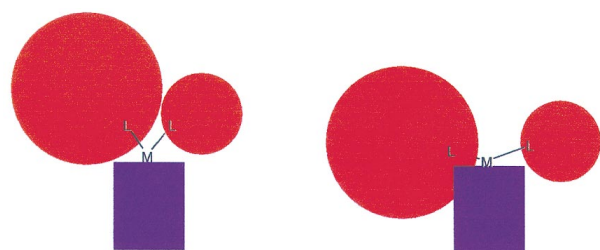
**Table 5** Average ligand bite angles compiled from crystal structures (standard deviation in parentheses, see Table 1 for details)

dppf 96° (2°)	dppb 98° (5°)	dppp 91° (2°)	dppe 85° (3°)	dppm 72° (2°)	dpp-benzene 83° (3°)
( <i>S,S</i> )-DUPHOS-Me 83°	DIOP 98°(5°)	BINAP 92°(3°)	( <i>R,S</i> )-BPPRA 100.47° <sup>65</sup>	( <i>R,S</i> )-BPPFA 98.79° <sup>71</sup>	

**Table 6** Cross-coupling of 2-butylmagnesium chloride with bromobenzene in diethyl ether. Conditions: 0.04 mmol catalyst, 8 mmol Grignard reagent and 4 mmol bromobenzene in 20 ml ether,  $T = 20\text{ }^{\circ}\text{C}$ 

Ligand	Bite angle/ $^{\circ}$	t.o.f. <sup>a</sup>	t/h	Conversion <sup>b</sup> (%)	Product (%)		
					Linear	Branched	Biphenyl
dppe <sup>c</sup>	85 (P–M–P <sub>2,315</sub> )	n.d.	48	4	0	0	n.d.
dppp <sup>c</sup>	91 (P–M–P <sub>2,315</sub> )	n.d.	24	67	69	31	n.d.
dppb <sup>c</sup>	98 (P–M–P <sub>2,315</sub> )	n.d.	8	98	51	25	n.d.
dppf	96 (P–M–P <sub>2,315</sub> )	79	2	100	95	2	3
DPEphos	102.2 ( $\beta_n$ )	181	2	100	98	1	1
Sixantphos	108.7 ( $\beta_n$ )	36	16	58.8	67	17	16
Thixantphos	109.4 ( $\beta_n$ )	24	16	36.5	51	17	32
Xantphos	111.7 ( $\beta_n$ )	24	16	23.6	41	19	40

n.d. = Not determined; ligand bite angles from Table 2. <sup>a</sup> Initial turnover frequency [ $\text{mol}(\text{mol Pd})^{-1}\text{h}^{-1}$ ], determined after 5 min of reaction time. <sup>b</sup> Conversions based on bromobenzene. <sup>c</sup> Results from ref. 13.

**Scheme 8** The interaction between the substrate (represented as dark rectangle) co-ordinated to a metal centre and the (chiral) ligand's substituents (circles) increases with the L–M–L bite angle.

activation energy in a system with an unconstrained bite angle (Fig. 5).

Portnoy and Milstein<sup>41</sup> observed that the oxidative addition of aryl chlorides to (P–P)Pd<sup>0</sup> species is faster with decreasing ligand bite angles, and Brown and Guiry<sup>42</sup> concluded that the rate of reductive elimination in palladium catalysed Grignard cross coupling reactions increases with the bite angle. Earlier, Yamamoto and co-workers<sup>57</sup> had found that ethane was

eliminated from [NiMe<sub>2</sub>(dppp)] 46 times faster than from [NiMe<sub>2</sub>(dppe)] (ligand bite angles of 91 and 85°, respectively). Using DIOP (98°), the elimination of RCN from [Pd(R)(CN)-(P–P)] (R = CH<sub>2</sub>SiMe<sub>3</sub>) is 10000 times faster than that using the dppe ligand (85°).<sup>58</sup> These results can be understood with the Walsh diagram (Fig. 4) discussed above. The oxidative addition is supported by ligands having smaller bite angles, because they increase the electron density on the (P–P)Pd<sup>0</sup> metal centre. Larger bite angles which go along with decreased electron density on the metal make the reductive elimination easier.

A correlation between increasing diphosphine ligand bite angles and rate or selectivity has also been observed in cobalt- or nickel-catalysed cross coupling reactions, for example in the coupling of arylboronic acids with aryl halides<sup>59</sup> or in the reaction of catechol–borane with various dienes.<sup>60</sup>

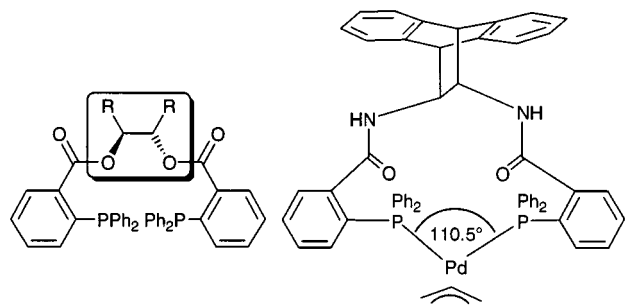
An important point to keep in mind when discussing rates and selectivities in Pd-catalysed reactions is the catalyst stability. Palladium(0) species tend to form metallic palladium (palladium black), especially if reactions are performed at higher temperatures. This decreases the activity of the catalyst if metallic palladium does not catalyse the reaction and the

selectivity if it does. The catalyst concentration might also be diminished by equilibria involving the starting material used,<sup>6</sup> and solvent effects, albeit poorly understood, have a strong influence in many catalytic reactions. The overall effect of a single parameter such as the ligand bite angle may become ambiguous if the catalyst concentration and its activity are both a function of this parameter. The bite angle effect in palladium catalysed reactions of aryl halides with amines is a good example.<sup>8</sup> The ambiguous overall picture is probably due to a combination of elementary steps affected differently by changes of the ligand bite angle.

### Enantioselective reactions

From a mechanistic point of view, reactions involving chiral centres are very similar to those not involving chirality. Factors determining rate, selectivity and the energy profile should be the same for both. A reaction is enantioselective if interactions between ligand and substrate during the catalytic reaction favour the formation of one of the product enantiomers. Interactions require proximity. Parts of the ligand have to be close to the active site of the catalyst. In most bidentate ligands the orientation of the interacting parts of the ligand with regard to the substrate co-ordinated to the metal atom is related to the ligand bite angle (Scheme 8).

Trost *et al.*<sup>61</sup> have designed a modular ligand system for allylic alkylation reactions: two 2-(diphenylphosphino)benzoic acid groups are attached to a chiral backbone. Palladium complexes of these ligands are very selective catalysts for the enantioselective substitution of small allylic substrates. The chiral pocket formed upon complexation to a metal centre can be fine tuned by varying the chiral diol/diamine used to form the backbone (Scheme 9). It was postulated that the opening of



**Scheme 9** A modular system to build ligands for asymmetric allylic alkylation reactions.

the bite angle is necessary for high chiral recognition<sup>61</sup> in allylic alkylation reactions. For one of the ligands the P–Pd–P angle in a [Pd(C<sub>3</sub>H<sub>5</sub>)(P–P)] complex was determined to be 110.5°.<sup>62</sup> From studying Corey–Pauling–Koltun (CPK) models, Trost and Murphy<sup>20</sup> had earlier concluded that “a larger ring of a chelating bidentate ligand leads to greater embracing of the allyl fragment by the metal template and consequently higher asymmetric induction.” Similarly, the regioselectivity in the (non-asymmetric) alkylation of 2-hexenyl acetate increases with an increasing ligand bite angle.<sup>63,64</sup>

Hayashi *et al.*<sup>65</sup> compared the selectivity of chiral ferrocene and ruthenocene based ligands BPPFA (P–M–P angle 98.79°) and BPPRA (P–M–P angle 100.47°) in asymmetric silylation and cyclisation reactions. Despite the small difference, the enantioselectivities obtained with BPPRA were up to 40% higher. In a series of spirobis(oxazoline) ligands the enantioselectivity in copper-catalysed Diels–Alder reactions was shown to increase with the (calculated) ligand bite angle.<sup>19</sup>

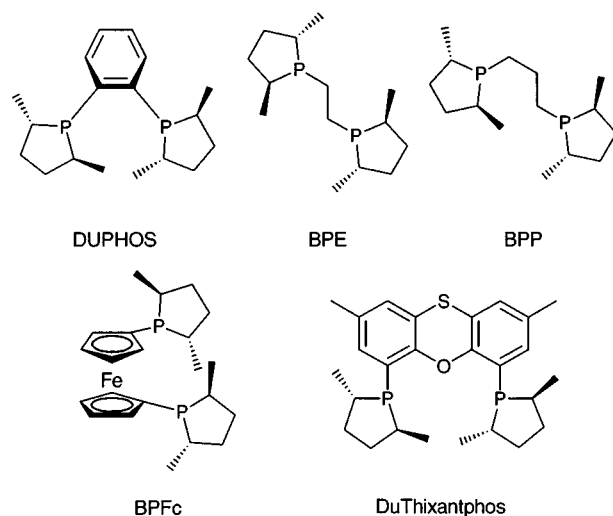
There are many asymmetric reactions where the bite angle effect might be important. Asymmetric hydrogenation is an example for a reaction of which the ligand bite angle has not been examined explicitly. Burk *et al.*<sup>66–69</sup> have prepared a series

**Table 7** The effect of the ligand bite angle on the enantioselectivity in rhodium catalysed homogenous hydrogenation reactions

Ligand	P–M–P <sup>a/o</sup>	e.e.			Ref.
		R = Ph	Me	H	
DUPHOS	83	99	98		68
BPE	85	91.4	85		68
BPP	98	60			66
BPFc	96			64	69
DuThixantphos	104	30			72

<sup>a</sup> For consistency reasons, all bite angles are those of non-chiral analogs (PPh<sub>2</sub>, see Scheme 9). Measured bite angles for DUPHOS and BPE in [Rh(COD)(P–P)]SbF<sub>6</sub> complexes are 84.72° and 83.3°,<sup>67</sup> respectively [ $r(\text{Rh}–\text{P}_{\text{av}})$  2.26 Å for both].

of ligands with two phospholane units carrying chiral groups attached to different backbones. Even though the substrates tested are not exactly the same, the selectivities observed clearly decrease with increasing ligand bite angle (Table 7, Scheme 10).



**Scheme 10** Bisphospholane ligands with different bite angles.

It would certainly be wrong to generalise that ligands with bite angles of 85° form better hydrogenation catalysts than those with larger angles. BINAP and DIOP for example, with ligand bite angles of 92 and 98°, can be as selective as DUPHOS. To develop new phospholane based ligands for the hydrogenation of olefins ligands with bite angles between 85 and 95° would probably be the best choice.

## 7 Conclusion

The ligand bite angle is a property that can be calculated from a series of crystal structures or from molecular modelling. Systematic searches in the Cambridge Crystallographic Database show that the P–M–P angles concentrate in narrow ranges for most transition metal complexes containing (P–P)M fragments. The average values calculated from crystal structures are in good agreement with ligand bite angles calculated with molecular mechanics, even if simplified parameters are employed for a “dummy metal atom” connecting the two phosphorus atoms. The ligand bite angle correlates with various spectroscopic properties of metal–diphosphine complexes and with the regio- or stereo-selectivity in a variety of catalytic reactions. In rhodium catalysed hydroformylation reactions, ligands with bite angles >100° favour the formation of linear aldehydes.

In many palladium catalysed reactions ligands such as dppf or dppp with bite angles around 100° give the best results in terms of activity and selectivity. In the case of palladium this can be explained by transition states between (four-co-ordinate) palladium(II) species with P–Pd–P angles around 90° and two- or three-co-ordinate palladium(0) species with P–Pd–P angles of probably 120–180°. Although the hypothesis will have to be substantiated, the examples discussed in this article indicate that there is an optimum bite angle for many catalytic systems.

A large number of (chiral) ligand backbones and of (chiral) PR<sub>2</sub> groups has been developed over the last decades. They can be combined to tailor an almost indefinite number of ligands. The ligand bite angle concept can help to determine the right one. Sharpless has been quoted “If you give me high rates of turnover, I can probably give you the selectivity later . . .”<sup>70</sup> A better understanding of the bite angle effect might be the key to both.

## 8 References

- 1 C. A. Tolman, *Chem. Rev.*, 1977, **77**, 313.
- 2 Science Citation Index Web of Science, www.isinet.com.
- 3 A. Fernandez, C. Reyes, M. R. Wilson, D. C. Woska, A. Prock and M. P. Giering, *Organometallics*, 1997, **16**, 342.
- 4 S. Joerg, R. S. Drago and J. Sales, *Organometallics*, 1998, **17**, 589.
- 5 E. C. Alyea and S. Q. Song, *Comments Inorg. Chem.*, 1996, **18**, 189.
- 6 C. Amatore, G. Broeker, A. Jutand and F. Khalil, *J. Am. Chem. Soc.*, 1997, **119**, 5176.
- 7 C. Amatore, A. Jutand and G. Meyer, *Inorg. Chim. Acta*, 1998, **273**, 76.
- 8 B. C. Hamann and J. F. Hartwig, *J. Am. Chem. Soc.*, 1998, **120**, 3694.
- 9 E. M. Vogl, J. Bruckmann, C. Krüger and M. W. Haenel, *J. Organomet. Chem.*, 1996, **520**, 249.
- 10 T. Hayashi, Y. Kawabata, T. Isoyama and I. Ogata, *Bull. Chem. Soc. Jpn.*, 1981, **54**, 3438.
- 11 Y. Kawabata, T. Hayashi and I. Ogata, *J. Chem. Soc., Chem. Commun.*, 1979, 462.
- 12 T. Hayashi, M. Konishi and M. Kumada, *Tetrahedron Lett.*, 1979, **21**, 1871.
- 13 T. Hayashi, M. Konishi, Y. Kobori, M. Kumada, T. Higuchi and K. Hirotsu, *J. Am. Chem. Soc.*, 1984, **106**, 158.
- 14 C. P. Casey, G. T. Whiteker, M. G. Melville, L. M. Petrovich, J. A. Gavney and D. R. Powell, *J. Am. Chem. Soc.*, 1992, **114**, 5535 and 10680.
- 15 M. Kranenburg, Y. E. M. van der Burgt, P. C. J. Kamer, P. W. N. M. van Leeuwen, K. Goubitz and J. Fraanje, *Organometallics*, 1995, **14**, 3081.
- 16 K. Yamamoto, S. Momose, M. Funahashi, S. Ebata, H. Ohmura, H. Komatsu and M. Miyazawa, *Chem. Lett.*, 1994, 189.
- 17 W. Goertz, P. C. J. Kamer, P. W. N. M. van Leeuwen and D. Vogt, *Chem. Commun.*, 1997, 1521.
- 18 M. Kranenburg, P. C. J. Kamer, P. W. N. M. van Leeuwen, D. Vogt and W. Keim, *J. Chem. Soc., Chem. Commun.*, 1995, 2177.
- 19 I. W. Davies, L. Gerena, L. Castonguay, C. H. Senanayake, R. D. Larsen, T. R. Verhoeven and P. J. Reider, *Chem. Commun.*, 1996, 1753.
- 20 B. M. Trost and D. J. Murphy, *Organometallics*, 1985, **4**, 1143.
- 21 P. Dierkes, S. Ramdeehul, L. Barloy, A. De Cian, J. Fischer, P. C. J. Kamer, P. W. N. M. van Leeuwen and J. A. Osborn, *Angew. Chem.*, 1998, **110**, 3299; *Angew. Chem., Int. Ed.*, 1998, **37**, 3116.
- 22 S. Ramdeehul, P. Dierkes, R. Aguado, P. C. J. Kamer, P. W. N. M. van Leeuwen and J. A. Osborn, *Angew. Chem.*, 1998, **110**, 3302; *Angew. Chem., Int. Ed.*, 1998, **37**, 3118.
- 23 T. Yoshida, K. Tatsumi and S. Otsuka, *Pure Appl. Chem.*, 1980, **52**, 713.
- 24 P. Hofmann, L. A. Perezmoya, O. Steigelmann and J. Riede, *Organometallics*, 1992, **11**, 1167.
- 25 C. P. Casey and G. T. Whiteker, *Isr. J. Chem.*, 1990, **30**, 299.
- 26 F. H. Allen, O. Kennard, D. G. Watson, L. Brammer, A. G. Orpen and R. Taylor, *J. Chem. Soc., Perkin Trans. 2*, 1987, S1.
- 27 A. G. Orpen, L. Brammer, F. H. Allen, O. Kennard, D. G. Watson and R. Taylor, *J. Chem. Soc., Dalton Trans.*, 1989, S1.
- 28 T. E. Müller and D. M. P. Mingos, *Transition Met. Chem.*, 1995, **20**, 533.
- 29 M. Sato, H. Shigeta, M. Sekino and S. Akasori, *J. Organomet. Chem.*, 1993, **458**, 199.
- 30 M. D. K. Boele and P. W. N. M. van Leeuwen, unpublished work.
- 31 A. G. Avent, R. B. Bedford, P. A. Chaloner, S. Z. Dewa and P. B. Hitchcock, *J. Chem. Soc., Dalton Trans.*, 1996, 4633.
- 32 M. Kranenburg, J. G. P. Delis, P. C. J. Kamer, P. W. N. M. van Leeuwen, K. Vrieze, N. Veldman, A. L. Spek, K. Goubitz and J. Fraanje, *J. Chem. Soc., Dalton Trans.*, 1997, 1839.
- 33 D. L. Thorn and R. Hoffmann, *J. Am. Chem. Soc.*, 1978, **100**, 2079.
- 34 B. B. Coussens, F. Buda, H. Oevering and R. J. Meier, *Organometallics*, 1998, **17**, 795.
- 35 L. Mole, J. L. Spencer, N. Carr and A. G. Orpen, *Organometallics*, 1991, **10**, 49.
- 36 S. Otsuka, *J. Organomet. Chem.*, 1980, **200**, 191.
- 37 J. Browning, M. Green, A. Laguna, L. E. Smart, J. L. Spencer and F. G. A. Stone, *J. Chem. Soc., Chem. Commun.*, 1975, 723.
- 38 J. Browning, M. Green, B. R. Penfold, J. L. Spencer and F. G. A. Stone, *J. Chem. Soc., Chem. Commun.*, 1973, 31.
- 39 P. Hofmann, H. Heiß and G. Müller, *Z. Naturforsch., B: Chem. Sci.*, 1987, **42**, 395.
- 40 S. A. Wander, A. Miedaner, B. C. Noll, R. M. Barkley and D. L. Dubois, *Organometallics*, 1996, **15**, 3360.
- 41 M. Portnoy and D. Milstein, *Organometallics*, 1993, **12**, 1665.
- 42 J. M. Brown and P. J. Guiry, *Inorg. Chim. Acta*, 1994, **220**, 249.
- 43 J. De Priest, G. Y. Zheng, C. Woods, D. P. Rillema, N. A. Mikirova and M. E. Zandler, *Inorg. Chim. Acta*, 1997, **264**, 287.
- 44 A. Miedaner, R. C. Haltiwanger and D. L. Dubois, *Inorg. Chem.*, 1991, **30**, 417.
- 45 S. Q. Song and E. C. Alyea, *Comments Inorg. Chem.*, 1996, **18**, 145.
- 46 K. Angermund, W. Baumann, E. Dinjus, R. Fornika, H. Görls, M. Kessler, C. Krüger, W. Leitner and F. Lutz, *Chem. Eur. J.*, 1997, **3**, 755.
- 47 A. G. Bell, W. Kozminski, A. Linden and W. von Philipsborn, *Organometallics*, 1996, **15**, 3124.
- 48 V. Tedesco and W. von Philipsborn, *Magn. Reson. Chem.*, 1996, **34**, 373.
- 49 M. J. Calhorda, J. M. Brown and N. A. Cooley, *Organometallics*, 1991, **10**, 1431.
- 50 C. K. Brown and G. Wilkinson, *J. Chem. Soc. A*, 1970, 2753.
- 51 D. Evans, J. A. Osborn and G. Wilkinson, *J. Chem. Soc. A*, 1968, 3133.
- 52 T. J. Devon, G. W. Phillips, T. A. Puckette, J. L. Stavinoha and J. J. Vanderbilt, *World Patent*, W087/07600, 1987.
- 53 C. P. Casey and L. M. Petrovich, *J. Am. Chem. Soc.*, 1995, **117**, 6007.
- 54 C. P. Casey, E. L. Paulsen, E. W. Beuttenmueller, B. R. Proft, L. M. Petrovich, B. A. Matter and D. R. Powell, *J. Am. Chem. Soc.*, 1997, **119**, 11817.
- 55 L. A. van der Veen, M. D. K. Boele, F. Bregman, P. C. J. Kamer, P. W. N. M. van Leeuwen, K. Goubitz, J. Fraanje, H. Schenk and C. Bo, *J. Am. Chem. Soc.*, 1998, **120**, 11616.
- 56 M. Kranenburg, P. C. J. Kamer and P. W. N. M. van Leeuwen, *Eur. J. Inorg. Chem.*, 1998, 155.
- 57 T. Kohara, T. Yamamoto and A. Yamamoto, *J. Organomet. Chem.*, 1980, **192**, 265.
- 58 J. E. Marcone and K. G. Moloy, *J. Am. Chem. Soc.*, 1998, **120**, 8527.
- 59 S. Saito, S. Ohtani and N. Miyaoura, *J. Org. Chem.*, 1997, **62**, 8024.
- 60 M. Zaidlewicz and J. Meller, *Tetrahedron Lett.*, 1997, **38**, 7279.
- 61 B. M. Trost, D. L. van Vranken and C. Bingel, *J. Am. Chem. Soc.*, 1992, **114**, 9327.
- 62 B. M. Trost, B. Breit, S. Peukert, J. Zambrano and J. W. Ziller, *Angew. Chem., Int. Ed. Engl.*, 1995, **34**, 2386.
- 63 M. Kranenburg, P. C. J. Kamer and P. W. N. M. van Leeuwen, *Eur. J. Inorg. Chem.*, 1998, 25.
- 64 R. J. van Haaren, H. Oevering, P. W. N. M. van Leeuwen, P. C. J. Kamer, J. N. H. Reek, G. P. F. van Strijdonck and B. B. Coussens, submitted for publication.
- 65 T. Hayashi, A. Ohno, S. J. Lu, Y. Matsumoto, E. Fukuyo and K. Yanagi, *J. Am. Chem. Soc.*, 1994, **116**, 4221.
- 66 M. J. Burk, J. E. Feaster and R. L. Harlow, *Tetrahedron: Asymmetry*, 1991, **2**, 569.
- 67 M. J. Burk, J. E. Feaster and R. L. Harlow, *Organometallics*, 1990, **9**, 2653.
- 68 M. J. Burk, J. E. Feaster, W. A. Nugent and R. L. Harlow, *J. Am. Chem. Soc.*, 1993, **115**, 10125.
- 69 M. J. Burk and M. F. Gross, *Tetrahedron Lett.*, 1994, **35**, 9363.
- 70 S. Borman, *Chem. Eng.*, 1996, 4th November, 37.
- 71 T. Hayashi, M. Kumada, T. Higuchi and K. Hirotsu, *J. Organomet. Chem.*, 1987, **334**, 195.
- 72 P. Dierkes, U. Nettekoven and P. W. N. M. van Leeuwen, unpublished work.